Vortex Photon Model: Program for Experimental Verification

Dmitry Losinets

March 2026

Abstract

This work investigates a vortex-based model of the photon as an alternative approach to quantum electrodynamics (QED), grounded in the formal Kelvin–Voigt (K–V) mechanical analogy for Maxwell's equations derived in [1]. While mathematically consistent with the Jones formalism for polarization in describing transverse *far-field* components, the model makes distinct, falsifiable predictions: a non-zero longitudinal mechanical displacement of vacuum-medium elements in the *near field* of a propagating photon-vortex, detectable at sub-wavelength distances from the beam axis. The far-field propagating mode is strictly transverse, as required by the Coulomb gauge that the K–V incompressibility condition imposes exactly. The article focuses on designing critical experiments to test these predictions, including near-field detection of longitudinal field structure and analysis of angular momentum transfer during photon absorption. Results from these experiments could either validate the model or reinforce the standard QED framework.

1 Introduction

Standard quantum electrodynamics (QED) represents one of the most accurate and well-verified physical theories, whose predictions have been brilliantly confirmed experimentally [2, 3]. The mathematical apparatus of QED, based on the concept of gauge fields, has no equal in its predictive power [4, 5]. However, its abstract nature and lack of intuitive mechanical analogies for describing quantum objects such as photons continue to stimulate the search for alternative interpretations and models that can bridge the gap between mathematical formalism and intuitive understanding [6].

This work explores the possibility of mechanical description of photons within the framework of a vortex model of the quantum vacuum, as systematically presented in [1]. The fundamental basis of this approach — established rigorously in [1] and summarised for the reader's convenience in Sec. 2.1 below — is that a dilute assembly of compact vortex rings in a Kelvin–Voigt (K–V) viscoelastic medium obeys equations formally identical to Maxwell's equations. Specifically, the K–V constitutive law combined with incompressibility yields the correspondence between the vector potential $\mathbf{A}$ and the solenoidal velocity field $\mathbf{u}$ of the medium (eq. (6)):

$$\mathbf{A} = R\,\mathbf{u}, \qquad R \equiv \tau_{\mathrm{KV}} = \frac{\eta_0}{G}, \tag{1}$$

where η_0 is the dynamic viscosity of the medium and $G \sim \rho_0\Gamma^2/r_0^2$ is the effective shear modulus arising from the Tkachenko mechanism of vortex-ring collective elasticity (eq. (2)). The conversion constant R equals the K–V mechanical relaxation time and is in principle measurable from the fluid properties of the medium (eq. (4)).

The aim of this article is not to refute QED, but to demonstrate that this model: (1) is self-consistent within its framework — its mathematical description for transverse *far-field* components reduces to the known Jones formalism for polarization [7]; (2) is mechanically grounded — the correspondence $\mathbf{A} = R\mathbf{u}$ is *derived* from the K–V constitutive law in [1]; (3) differs from standard theory through fundamentally testable predictions, the most important of which is the existence of a *near-field* longitudinal displacement component in the vacuum medium surrounding a propagating photon, at sub-wavelength distances from the beam axis [8, 9]; and (4) is falsifiable — it offers specific experiments whose results can unambiguously confirm or refute its key postulates [10].

Thus, the work focuses on developing and describing critical experiments designed to test this hypothesis and quantitatively evaluate its predictions [8, 9].

2 Theoretical Framework

2.1 Summary of the Kelvin–Voigt mechanical analogy

We collect here the key results of [1] that are used throughout this paper; readers familiar with that work may skip to Sec. 2.2.

Vortex-ring medium and shear modulus. A dilute assembly of compact Hill-type vortex rings in an incompressible fluid acts as a viscoelastic Kelvin–Voigt (K–V) solid. Each ring of circulation Γ and core radius r_0 provides an elastic restoring force upon deformation; the collective (Tkachenko) back-reaction of neighbouring rings yields the effective shear modulus [11]

$$G = \frac{\rho_0 \Gamma^2}{4\pi r_0^2} \quad \text{(dominant Tkachenko contribution)}, \tag{2}$$

with an additional shape-stability contribution of similar order ($G_{\text{shape}} \approx 1.94\, G_{\text{Tk}}$), so $G \sim \rho_0 \Gamma^2 / r_0^2$ in both cases. The K–V constitutive relation for the deviatoric stress is

$$\boldsymbol{\tau} = 2G\,\mathbf{E}(\mathbf{d}) + 2\eta_0\,\mathbf{D}(\mathbf{u}), \tag{3}$$

where $\mathbf{d}$ is the displacement field, $\mathbf{u} = \partial_t \mathbf{d}$ the velocity, and $\eta_0 = \rho_0 \nu$ the dynamic viscosity. The shear-wave speed and K–V relaxation time are

$$c \equiv \sqrt{G/\rho_0}, \qquad R \equiv \tau_{\text{KV}} = \frac{\eta_0}{G} = \frac{\nu}{c^2}. \tag{4}$$

Wave equation for the vector potential. For the solenoidal velocity field $\mathbf{u}$ (guaranteed by incompressibility $\nabla \cdot \mathbf{u} = 0$), the K–V constitutive law (3) inserted into the linearised momentum balance gives the damped shear-wave equation

$$\partial_{tt}\mathbf{u} - c^2 \nabla^2 \mathbf{u} = \nu \nabla^2 \partial_t \mathbf{u}. \tag{5}$$

The electromagnetic vector potential is identified as

$$\mathbf{A} \equiv R\,\mathbf{u}, \tag{6}$$

so that $\mathbf{A}$ satisfies the identical equation

$$\partial_{tt}\mathbf{A} - c^2\nabla^2\mathbf{A} = \nu\nabla^2\partial_t\mathbf{A}. \tag{7}$$

This is an *exact consequence* of the K–V constitutive law, not an additional assumption.

Coulomb gauge from incompressibility. Since $\mathbf{A} = R\mathbf{u}$ and $\nabla\cdot\mathbf{u} = 0$ (incompressibility),

$$\nabla\cdot\mathbf{A} = R\,\nabla\cdot\mathbf{u} = 0. \tag{8}$$

The Coulomb gauge condition holds *identically*, as a direct consequence of the incompressible K–V medium, without being imposed by hand.

Circulation invariant and hydrodynamic charge. By Kelvin's circulation theorem, the circulation $\Gamma = \oint_C \mathbf{u}\cdot d\mathbf{l}$ around any loop encircling a vortex tube is conserved to $O(\delta)$ where $\delta = \nu/(cL) \ll 1$ is the viscosity parameter. The hydrodynamic charge—the circulation invariant of the vortex—is

$$Q \equiv \rho_0\, r_0\, \Gamma, \tag{9}$$

with the sign fixed by the right-hand rule orientation of C. Quantisation of circulation, $\Gamma_n = nh/m_{\text{vac}}$, mirrors the discreteness of electric charge.

2.2 Electromagnetic potentials and Coulomb gauge

In the Coulomb gauge ($\nabla\cdot\mathbf{A} = 0$, $\phi = 0$ for source-free fields), the field–potential relations reduce to [12]:

$$\mathbf{E} = -\frac{\partial\mathbf{A}}{\partial t}, \qquad \mathbf{B} = \nabla\times\mathbf{A}. \tag{10}$$

These completely describe free electromagnetic waves. In QED the same relations hold for field operators $\hat{\mathbf{E}} = -\partial_t\hat{\mathbf{A}}$; the single-photon state $|1_{\mathbf{k},\lambda}\rangle = \hat{a}^{+}_{\mathbf{k},\lambda}|0\rangle$ has vanishing field expectation values but well-defined operator structure [4, 13].

2.3 Vortex model correspondence

Within the K–V vortex model [1] (see Sec. 2.1), a photon is a compact vortex ring with a localized core propagating through the viscoelastic medium [14, 15]. The vorticity is concentrated near the ring centreline and decays smoothly to negligible values at distances large compared to the core size; the specific core profile does not affect the integral quantities (circulation, orbital radius) on which the model relies. The field–velocity correspondence $\mathbf{A} = R\,\mathbf{u}$ (eq. (6)) is *derived* from the K–V constitutive law (3) and incompressibility, as shown in Sec. 2.1.

For a fluid element on the ring with tangential velocity $\mathbf{V}$:

$$\mathbf{V} = \frac{\mathbf{A}}{R}, \qquad R = \tau_{\text{KV}} = \frac{\eta_0}{G}. \tag{11}$$

Incompressibility gives the Coulomb gauge $\nabla\cdot\mathbf{A} = 0$ exactly. The electric field corresponds to (minus) the fluid acceleration:

$$\mathbf{E} = -R\,\frac{\partial\mathbf{V}}{\partial t}. \tag{12}$$

For circular motion on a ring of major radius ρ, the centripetal acceleration has magnitude $|\partial_t\mathbf{V}| = V^2/\rho = \omega^2\rho$, giving $|\mathbf{E}| = R\omega^2\rho$.

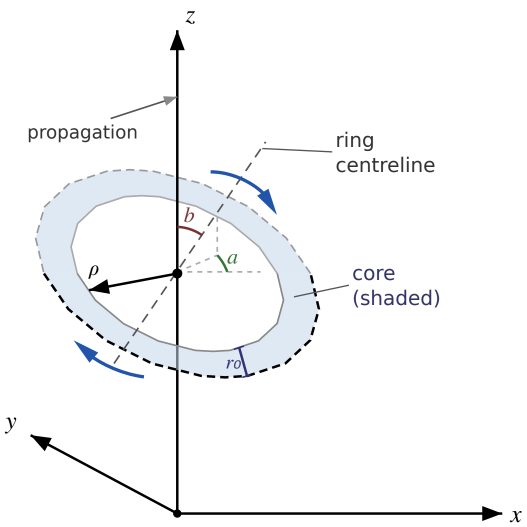

Figure 1: Geometry of the photon-vortex ring. The major radius ρ scales as $\omega^{-1/2}$ (eq. (14)); the core size r_0 sets the near-field range (eq. (16)). Angles (a, b) parameterize the vortex orientation and determine the polarization state (Sec. 2.6.2).

2.4 Photon energy from quantum circulation

The rotational frequency ω of fluid elements is identified with the photon angular frequency. The Onsager–Feynman quantization condition for circulation in a superfluid-like medium [16, 17, 18] requires:

$$\Gamma_n = n\,\frac{h}{m_{\rm vac}}, \quad n = 1, 2, \ldots, \tag{13}$$

where $m_{\rm vac}$ is an effective mass scale of the vacuum medium. For a fluid element on the ring of major radius ρ with tangential speed $V = \omega\rho$, the circulation is $\Gamma = 2\pi\rho V = 2\pi\omega\rho^2$. Setting $n = 1$ in (13):

$$2\pi\omega\rho^2 = \frac{h}{m_{\rm vac}} \quad \Longrightarrow \quad \rho(\omega) = \sqrt{\frac{\hbar}{m_{\rm vac}\,\omega}}. \tag{14}$$

Higher-frequency photons correspond to smaller vortex rings: $\rho \propto \omega^{-1/2}$. The multi-quantum generalisation ($n > 1$, same ρ) gives allowed frequencies $\omega_n = n\hbar/(m_{\rm vac}\rho^2) = n\omega_1$, so the energy spectrum is:

$$E_n = \hbar\omega_n = n\hbar\omega, \tag{15}$$

reproducing the Planck–Einstein relation from the vortex quantization condition alone. A complete quantitative check—computing the K–V elastic energy of the ring and verifying $E_{\rm ring} = \hbar\omega$—would fix $m_{\rm vac}$ in terms of c, G, and η_0, and remains an open problem.

2.5 Identification of the vortex core radius

The quantitative experimental predictions depend on the vortex core size r_0, which sets the transverse scale of the near-field longitudinal component. In classical vortex dynamics r_0 is a free parameter; in the K–V medium it is set by the coherence length of the medium.

Pending a first-principles derivation from the K–V elastic energy, we adopt the estimate

$$r_0 \lesssim \frac{\lambda}{2} = \frac{\pi c}{\omega}, \tag{16}$$

motivated as follows. The near-field displacement $r_z \propto \sin b$ must vanish at distances much larger than λ (otherwise it would contribute to the propagating wave mode, violating the Coulomb gauge). The largest core size consistent with sub-wavelength confinement is therefore $r_0 \sim \lambda/2$. A lower bound $r_0 \gtrsim \mathring{\lambda} = \lambda/(2\pi)$ is set by the photon's quantum coherence length (reduced wavelength). Thus

$$\frac{\lambda}{2\pi} \lesssim r_0 \lesssim \frac{\lambda}{2}. \tag{17}$$

For visible light ($\lambda \approx 500\,\mathrm{nm}$) this gives a concrete experimental target:

$$80\,\mathrm{nm} \lesssim r_0 \lesssim 250\,\mathrm{nm}. \tag{18}$$

Near-field probes with apertures $\sim$ 50–100 nm can reach this regime.

2.6 Jones formalism for vortex-ring polarization

Consider a thin-walled vortex ring of major radius ρ (distinct from the core radius r_0 and the conversion constant $R = \tau_{\mathrm{KV}}$) whose centre of mass propagates with velocity V along z. Each fluid element on the ring moves with constant tangential speed in a circular orbit whose plane is specified by the orientation angles (a, b): a is the azimuthal rotation about z, and b is the tilt of the ring plane away from the xy-plane.

2.6.1 Vortex-ring trajectory in the laboratory frame

In the vortex's own frame a fluid element on the ring traces a circle in the xy-plane with phase $\theta = \omega t + \varphi$, where φ is the element's initial phase ($\varphi = 0$ for the element on the x-axis at $t = 0$):

$$\mathbf{r}_{\mathrm{loc}} = \rho\big(\cos\theta,\ \sin\theta,\ 0\big). \tag{19}$$

Transforming to the laboratory frame applies the inverse rotations in reverse order, $\mathbf{r}_{\mathrm{global}} = \mathcal{R}_z(-a)\,\mathcal{R}_x(-b)\,\mathbf{r}_{\mathrm{loc}}$, with

$$\mathcal{R}_x(-b) = \begin{bmatrix} 1 & 0 & 0 \\ 0 & \cos b & \sin b \\ 0 & -\sin b & \cos b \end{bmatrix}, \qquad \mathcal{R}_z(-a) = \begin{bmatrix} \cos a & \sin a & 0 \\ -\sin a & \cos a & 0 \\ 0 & 0 & 1 \end{bmatrix}. \tag{20}$$

Carrying out the matrix products yields the trajectory components:

$$r_x = \rho\big[\cos a \cos\theta - \sin a \cos b \sin\theta\big], \tag{21}$$

$$r_y = \rho\big[\sin a \cos\theta + \cos a \cos b \sin\theta\big], \tag{22}$$

$$r_z = \rho\ \sin b \sin\theta. \tag{23}$$

As a consistency check: at $\theta = 0$ the element is at $\rho(\cos a, \sin a, 0)$, the position after the two applied rotations; at $\theta = \pi/2$ it reaches $\rho(-\sin a \cos b,\, \cos a \cos b,\, \sin b)$.

To identify the propagating electromagnetic mode we adopt the convention $\theta = -\omega t$ (right-hand circulation viewed from $+z$; reversing to $\theta = +\omega t$ corresponds to $b \to \pi - b$, see Sec. 2.6.2) and form the analytic signal in the transverse plane. Substituting into the xy-components and collecting the identities $\cos\theta - i\sin\theta = e^{-i\theta}$ and $\sin\theta + i\cos\theta = ie^{-i\theta}$ gives

$$X = e^{-i\theta}\big[\cos a - i\sin a\cos b\big], \tag{24}$$

$$Y = e^{-i\theta}\big[\sin a + i\cos a\cos b\big]. \tag{25}$$

Defining the Jones complex amplitudes

$$J_x = \cos a - i\sin a\cos b, \tag{26}$$

$$J_y = \sin a + i\cos a\cos b, \tag{27}$$

and setting $\theta = -\omega t$ yields $X = e^{i\omega t}J_x,\ Y = e^{i\omega t}J_y$, with amplitudes and phases

$$E_x = |J_x|, \quad \varphi_x = \arg J_x = -\arctan(\tan a\cos b), \tag{28}$$

$$E_y = |J_y|, \quad \varphi_y = \arg J_y = -\arctan(\cot a\cos b), \tag{29}$$

and $Z = 0$. The $Z = 0$ result is not a trivial projection artefact: K–V incompressibility ($\nabla\cdot\mathbf{u} = 0$) imposes the Coulomb gauge ($\nabla\cdot\mathbf{A} = 0$), which together with the source-free wave equation forces any propagating solution to be transverse, so the xy-projection of the vortex trajectory is exactly the propagating far-field mode. The physical z-displacement $r_z = \rho\sin b\sin\theta \neq 0$ for $b \neq 0$ is a non-propagating near-field component confined to $|\mathbf{r} - \mathbf{r}_{\text{vortex}}| \lesssim r_0$ and discussed in Sec. 2.6.3.

We thus obtain complete correspondence with the Jones formalism [7]. The mapping $(a, b) \mapsto (J_x, J_y)$ is not one-to-one: parameter pairs (a, b) and $(a+\pi, -b)$ yield the same Jones vector up to an overall phase, so the vortex orientation is determined by the Jones state only up to this equivalence.

2.6.2 Correspondence between vortex orientation and polarization state

The two-parameter family (a, b) spans the full Poincaré sphere. The tilt angle b controls the ellipticity of the polarization: $b = \pi/2$ places the vortex ring edge-on with respect to the propagation direction (linear polarization), while $b = 0$ or $b = \pi$ places it face-on (circular polarization, with opposite handedness). The azimuthal angle a sets the orientation of the polarization ellipse.

The correspondence is verified by direct substitution:

- At $b = 0$: $J_x = e^{-ia}$, $J_y = ie^{-ia}$, so $(J_x, J_y) \propto (1, i)$ — **right circular**, independent of a.
- At $b = \pi$: $J_x = e^{ia}$, $J_y = -ie^{ia}$, so $(J_x, J_y) \propto (1, -i)$ — **left circular**.
- At $b = \pi/2$: $J_x = \cos a$, $J_y = \sin a$ (both real) — **linear**, at orientation angle a.
- General $0 < b < \pi/2$ or $\pi/2 < b < \pi$: **elliptical**.

The principal cases are collected in Table 1, and Fig. 2 maps the (a, b) parameters onto the Poincaré sphere. The third Stokes parameter is $S_3 = \cos b$, so the degree of circular polarization is read off directly from the vortex tilt angle.

Table 1: Vortex orientation parameters (a, b) and corresponding polarization states.

a	b	Polarization state
0	$\pi/2$	Linear, horizontal (x)
$\pi/2$	$\pi/2$	Linear, vertical (y)
$\pi/4$	$\pi/2$	Linear, 45
any	0	Right circular
any	π	Left circular
general	$0 < b < \pi,\ b \neq \pi/2$	Elliptical

2.6.3 Near-field structure: the longitudinal displacement component

The derivation above shows that the *transverse projection* (XY plane) of the vortex-ring trajectory maps exactly to the Jones 2-component vector, establishing that the *propagating* electromagnetic mode is strictly transverse. This is entirely consistent with the K–V model: incompressibility ($\nabla \cdot \mathbf{u} = 0$) implies the Coulomb gauge $\nabla \cdot \mathbf{A} = 0$ exactly (eq. (8)), which together with the source-free Maxwell equations in the exterior gives $\nabla \cdot \mathbf{E} = 0$, i.e. no longitudinal propagating component.

However, for a vortex ring with tilt angle $b \neq 0$, the z-coordinate of a fluid element on the ring surface reads (eq. (23)):

$$r_z = \rho \sin(b) \sin(\theta), \qquad \theta = \omega t + \varphi, \tag{30}$$

which is *non-zero.* This z-oscillation represents a **near-field longitudinal displacement** of the vacuum medium within the vortex core region ($|\mathbf{r} - \mathbf{r}_{\text{vortex}}| \lesssim r_0$). It does not propagate as a wave mode (it is suppressed at distances $\gg r_0$ by the incompressibility constraint), but it *is* present in the immediate vicinity of the photon-vortex.

Crucially, Coulomb gauge does not prohibit $A_z \neq 0$ pointwise: it only requires $\nabla \cdot \mathbf{A} = 0$. Near the vortex core, $A_z = R u_z \neq 0$ while $\partial_z A_z$ is compensated by $\partial_x A_x + \partial_y A_y$ to maintain the divergence-free condition. The resulting near-field $E_z = -\partial_t A_z - \partial_z \phi \neq 0$ is analogous to the longitudinal near-field components of an oscillating electric dipole.

Contrast with standard QED: In standard QED a free photon in vacuum has no near-field structure at sub-wavelength distances (there is no physical medium and no vortex topology). Therefore the existence of a detectable near-field E_z at transverse distances $\Delta r \lesssim r_0$ from the photon path is a *falsifiable signature unique to the vortex model.*

3 Experimental Verification of the Model

3.1 Near-field Search for Longitudinal Displacement Component

Core distinction:

- **Standard model:** Electromagnetic waves in vacuum are strictly transverse everywhere for a free photon propagating away from any physical objects or boundaries. The vectors $\mathbf{E}$ and $\mathbf{B}$ are perpendicular to $\mathbf{k}$; no sub-wavelength longitudinal near-field structure exists in the absence of a physical medium, scatterer, or aperture.

- **Vortex model:** The far-field propagating mode is transverse (Jones formalism, Coulomb gauge from K–V incompressibility, Sec. 2.6.3). However, the vortex ring

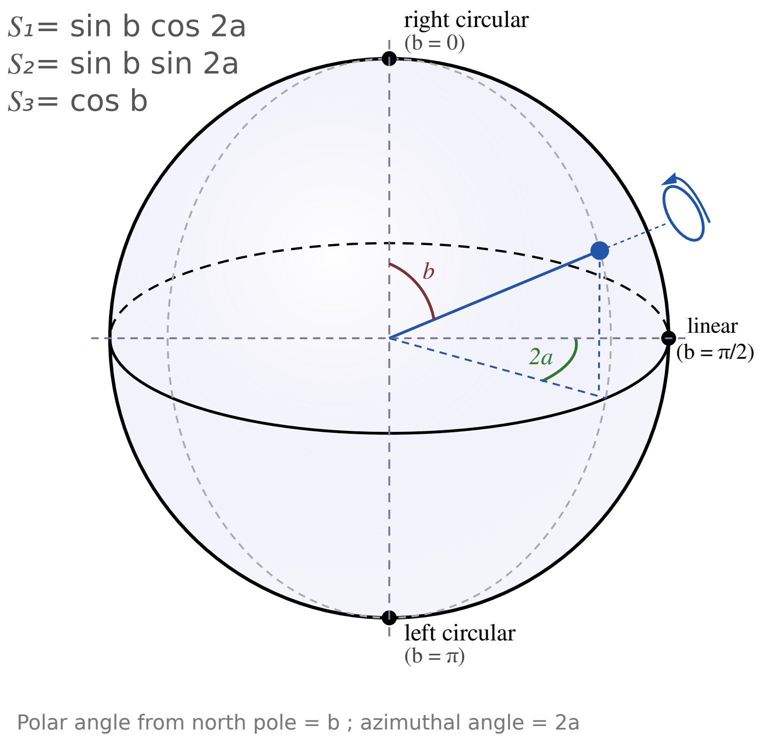

Figure 2: Poincaré sphere representation of the vortex orientation parameters (a, b). The polar angle from the north pole equals b; the azimuthal angle equals $2a$.

has a non-zero longitudinal displacement $r_z = \rho \sin(b)\sin(\omega t)$ for tilt angle $b \neq 0$, producing a near-field longitudinal electric component $E_z \neq 0$ at transverse distances $\Delta r \lesssim r_0$ from the photon path. This is an *evanescent* near-field effect, not a propagating mode.

Critical experimental requirement: The probe must couple to the photon field at **sub-wavelength transverse distance** $\Delta r \lesssim r_0$ from the beam axis, in the range 80–250 nm for visible light (eq. (18)). A conventional scanning near-field optical microscope (SNOM) is not suitable for probing free photons in vacuum: the tip perturbs or absorbs the photon rather than probing it non-destructively. Instead, we propose **photon-induced near-field electron microscopy (PINEM)** [19].

Setup: An ultrashort laser pulse (pump, wavelength λ, controlled polarization) is focused into a collimated beam in vacuum. A synchronised pulsed electron beam (probe, kinetic energy ∼100–300 keV) travels *parallel* to the laser axis $\hat{z}$ at controlled transverse offset Δr (electron trajectory: $(0, \Delta r, v_e t)$). In the PINEM interaction, the electron exchanges energy quanta $\hbar\omega$ with the optical field; for an electron of velocity v_e along z, the coupling constant is [19]:

$$g(\Delta r) \propto \int_{-\infty}^{\infty} E_z(0,\, \Delta r,\, z;\; t{=}z/v_e)\, e^{i\omega z/v_e}\, dz, \tag{31}$$

where E_z is the field component along the common propagation axis z. For a strictly transverse wave in vacuum, $E_z = 0$ everywhere and $g = 0$. The vortex model predicts

$E_z \neq 0$ at $\Delta r \lesssim r_0$, producing a non-zero coupling that scales as $\sin b$ (from eq. (23)) and decays on scale r_0 in Δr.

Procedure: Scan Δr from $\sim 0.1\lambda$ to $\sim 2\lambda$, recording the electron energy-loss spectrum (sidebands at $\pm n\hbar\omega$) for each impact parameter. Extract the PINEM coupling constant $|g(\Delta r)|^2$ from the sideband intensities. Repeat for linearly polarized ($b = \pi/2$) and circularly polarized ($b = 0$) pump beams.

Control: (1) Compare coupling profiles for linear vs. circular polarization. The vortex model predicts $|g|^2 \propto \sin^2 b$: maximum for linear ($b = \pi/2$), zero for circular ($b = 0$); standard QED predicts no polarization dependence of any anomalous E_z signal. (2) Use a reference geometry with the electron beam *on-axis* to characterise the background from the standard transverse field interaction.

Experimental challenge: Standard PINEM experiments rely on a material nanostructure (metal tip, nanoparticle, or aperture) to provide near-field enhancement that mediates the electron–photon coupling. For free photons propagating in open vacuum with no scatterer present, the only source of a longitudinal component is the photon-vortex near-field itself, so the coupling is expected to be far weaker than in surface-enhanced PINEM geometries. Detecting it will require laser-pulse energies and electron-beam currents near the upper limits of current experimental capability, together with careful subtraction of the on-axis reference signal arising from the standard transverse-field interaction. This challenge is, however, precisely what makes the experiment critical: a polarization-dependent residual at $\Delta r \lesssim r_0$ in the *absence* of any material scatterer would be unambiguous evidence for the near-field structure predicted by the vortex model and could not be attributed to surface-plasmon or aperture-diffraction artefacts.

Expected result according to standard theory: The PINEM coupling $|g(\Delta r)|^2$ is determined by the transverse field components $E_\perp$ only, falling off as a standard Bessel function of Δr, with no dependence on polarization ellipticity. Negative result (no anomalous polarization-dependent component) refutes the near-field prediction of the vortex model.

Expected result according to vortex model: An anomalous contribution to $|g(\Delta r)|^2$ at $\Delta r \lesssim r_0$, scaling as $\sin^2 b$ (vanishing for circular polarization, maximal for linear), and falling off on a scale $\sim r_0 \sim \mathring{\lambda}$ beyond the core region.

3.2 Angular Momentum Transfer and Vortex Topology at Photon Absorption

Core distinction:

- **Standard model:** A photon is a massless particle with spin 1, obeying conservation laws of energy, momentum, and angular momentum [20]. Its creation and absorption are point-like interaction acts in quantum field theory. The spin angular momentum $\pm\hbar$ is transferred to the absorbing atom as an internal (electronic) excitation, not as mechanical rotation of the atom's centre of mass.

- **Vortex model:** A photon is a compact vortex ring with circulation Γ conserved by Kelvin's theorem to order $\delta = \nu/(cL) \ll 1$ (Sec. 2.1). The charge analogue $Q = \rho_0 r_0 \Gamma$ (eq. (9), the circulation invariant) characterises the topological content of the photon. Upon absorption, the vortex topology must be either transferred to the absorbing atom/molecule or shed into the surrounding K–V medium. Both scenarios produce observable signatures distinct from QED: the absorbed angular momentum has a mechanical (orbital) component tied to the spatial extent of the vortex ring, not purely to the internal electronic degree of freedom.

Experiment description: Probe the mechanical recoil and angular momentum distribution during single-photon absorption in an isolated atom/ion.

Setup: An ion or atom cooled to ultralow temperatures and trapped in an ion trap (Paul or Penning type). A source of single photons (e.g., quantum dot or cavity QED source) emitting photons with known angular momentum (circularly polarized, $b = 0$: vortex ring in XY plane, spin axis along propagation direction).

Procedure: Observe the full quantum state of the ion after photon absorption. According to standard theory, the ion receives linear recoil $p = \hbar k$ and its internal angular momentum changes by $\pm\hbar$ (spin). The vortex model predicts an *additional* mechanical orbital angular momentum component proportional to $\Gamma r_0 \sim \hbar$ transferred from the vortex topology, potentially causing centre-of-mass rotation of the trapped ion about the beam axis, in excess of what QED predicts from the standard spin-to-orbit coupling.

Control: (1) Compare the result for circularly polarized ($b = 0$, ring in XY plane, spin axis along z) vs. linearly polarized ($b = \pi/2$, ring tilted, no spin component along z) photons. (2) Verify that the total angular momentum balance is satisfied: any excess orbital angular momentum transferred to the ion must be absent in the linearly polarized case.

Expected result according to standard theory: The change in the ion's mechanical angular momentum will equal the photon's spin ($\pm\hbar$) through standard spin-orbit coupling, with no anomalous centre-of-mass rotation. Negative result refutes the vortex model.

Expected result according to vortex model: Photon absorption will cause a measurable orbital recoil whose magnitude scales with the vortex core radius r_0 and circulation $\Gamma = Q/(\rho_0 r_0)$. The effect should vanish for linear polarization and be maximal for circular polarization.

Note on the quantitative prediction: The orbital angular momentum $L_{\text{orb}} \propto \Gamma r_0$ contains the undetermined parameter m_{vac} (via $\Gamma = h/m_{\text{vac}}$ and $r_0 \gtrsim \hbar/(m_{\text{vac}}c)$, see Sec. 2.4). The prediction is therefore currently *parametric*: a specific numerical value awaits the determination of m_{vac} from the energy condition $E_{\text{ring}} = \hbar\omega$. If self-consistency requires $L_{\text{orb}} \sim \hbar$, present-day ion-trap experiments on laser-cooled ions (e.g. $^{40}Ca^+$) can resolve individual angular-momentum quanta $\hbar$ via motional sideband spectroscopy, placing this regime within reach. The discriminating observable is the *difference* in mechanical angular-momentum transfer for circular ($b = 0$) versus linear ($b = \pi/2$) polarization at equal ω and k: standard QED forbids any such difference, while the vortex model predicts it.

4 Conclusion

In this work, we have analyzed the vortex photon model grounded in the Kelvin–Voigt mechanical analogy for Maxwell's equations developed in [1] and summarised in Sec. 2.1. The K–V framework provides a mechanical basis for the correspondence $\mathbf{A} = R\mathbf{u}$ (eq. (6)), where $R = \tau_{\text{KV}} = \eta_0/G$ (eq. (4)) is a measurable mechanical constant derived from the constitutive law (3).

We have shown that for transverse far-field components, the model reduces exactly to the Jones formalism, consistent with all known polarization phenomenology. More

Table 2: Summary of proposed experimental tests. Both predictions are derived from the K–V mechanical analogy of [1].

Experiment	**Standard Model Prediction**	**Vortex (K–V) Model Prediction**
PINEM coupling $\lvert g(\Delta r)\rvert^2$ at $\Delta r \lesssim r_0$ from beam	Coupling determined by transverse $E_\perp$ only; no polarization-ellipticity dependence	Anomalous coupling at $\Delta r \lesssim r_0 \sim \mathring{\lambda}$; zero for circular polarization ($b = 0$, $\sin^2 b = 0$), maximal for linear ($b = \pi/2$)
Photon absorption momentum transfer	Linear recoil $\hbar k$ + spin $\pm\hbar$ only; no anomalous c.o.m. rotation	Excess orbital c.o.m. angular momentum $\propto \Gamma r_0$; depends on polarization ellipticity

importantly, the K–V incompressibility condition *derives* the Coulomb gauge $\nabla \cdot \mathbf{A} = 0$ (eq. (8)), confirming that the propagating mode is strictly transverse — in full agreement with Maxwell's equations.

The principal novel prediction of the model concerns the **near-field structure** of the photon-vortex: for a tilted vortex ring ($b \neq 0$), a non-zero longitudinal displacement $r_z \neq 0$ exists at distances $\lesssim r_0$ from the vortex core. This produces a near-field longitudinal electric component $E_z \neq 0$ detectable at sub-wavelength transverse distances $\Delta r \lesssim r_0$ from the beam axis via photon-induced near-field electron microscopy (PINEM) [19]. Standard QED predicts no such near-field structure for free photons in vacuum.

We have proposed two falsifiable experimental schemes: (1) measurement of the PINEM coupling constant $|g(\Delta r)|^2$ as a function of transverse impact parameter and polarization ellipticity, sensitive to any anomalous longitudinal field at $\Delta r \lesssim r_0 \sim \mathring{\lambda}$; (2) measurement of excess orbital angular momentum transfer during single-photon absorption in a trapped ion, sensitive to the vortex circulation invariant $Q = \rho_0 r_0 \Gamma$.

Standard QED predicts strictly negative results in both experiments. Any confirmed positive result consistent with the model's quantitative predictions would have profound implications for our understanding of the physical vacuum. Conversely, negative results within achievable precision would falsify the vortex interpretation while still providing precision tests of the transverse nature of photons in vacuum and the completeness of QED angular momentum accounting.

Based on the requirement that the near-field be confined to sub-wavelength scales, we estimate $\mathring{\lambda} \lesssim r_0 \lesssim \lambda/2$, giving a concrete experimental target of 80–250 nm for visible light (Sec. 2.5). A first-principles derivation of r_0 from the K–V elastic energy of the vortex ring, and the associated quantitative prediction of the PINEM coupling amplitude, remain as key priorities for future work; this will require identifying m_{vac} in terms of c, G, and η_0 from the energy condition $E_{\text{ring}} = \hbar\omega$.

References

[1] D. S. Losinets. Maxwell's equations from vortex mechanics: A kelvin–voigt analogy. *Zenodo*, 2026.

[2] R. Loetzsch et al. Testing quantum electrodynamics in extreme fields using helium-like uranium. *Nature*, 625:673, 2024.

[3] R. G. Bullis et al. Ramsey spectroscopy of the 2s1/2 hyperfine interval in atomic hydrogen. *Physical Review Letters*, 2023.

[4] S. J. Brodsky. Review of quantum electrodynamics. Technical report, Stanford Linear Accelerator Center, 1992.

[5] S. G. Karshenboim. Precision physics of simple atoms: Qed tests, nuclear structure and fundamental constants. *Physics Reports*, 2005.

[6] S. Powers, G. Xu, et al. A statistical model for quantum spin and photon number states. *arXiv preprint*, 2024.

[7] M. Born and E. Wolf. *Principles of Optics: Electromagnetic Theory of Propagation, Interference and Diffraction of Light*. Cambridge University Press, 7th (expanded) edition, 1999.

[8] D. Sakhno, E. Koreshin, and P. A. Belov. Longitudinal electromagnetic waves with extremely short wavelength. *Physical Review B*, 104:L100304, 2021.

[9] D. Maluenda, M. Aviñoá, et al. Experimental estimation of the longitudinal component of a highly focused electromagnetic field. *Scientific Reports*, 2021.

[10] A. Zhakatayev and L. Tlebaldiyeva. Long-range longitudinal electric wave in vacuum radiated by electric dipole: Part i. *Radio Science*, 2020.

[11] V. K. Tkachenko. On vortex lattices. *Soviet Physics JETP*, 22:1282–1286, 1966.

[12] A. Blais and A. L. Grimsmo. Circuit quantum electrodynamics. *Reviews of Modern Physics*, 93:025005, 2021.

[13] M. Markiewicz, D. Kaszlikowski, P. Kurzyński, et al. From contextuality of a single photon to realism of an electromagnetic wave. *npj Quantum Information*, 5:5, 2019.

[14] L. Drori et al. Quantum vortices of strongly interacting photons. *Science*, 2023.

[15] J. P. Restrepo Cuartas and C. A. Flórez-Acosta. Dynamics of a quantum polariton vortex: Low-excitation scenario. *Physical Review B*, 110:155433, 2024.

[16] L. Onsager. Statistical hydrodynamics. *Nuovo Cimento Suppl.*, 6:279–287, 1949.

[17] R. P. Feynman. Application of quantum mechanics to liquid helium. In C. J. Gorter, editor, *Progress in Low Temperature Physics*, volume 1, pages 17–53. North-Holland, 1955.

[18] R. J. Donnelly. *Quantized Vortices in Helium II*. Cambridge University Press, 1991.

[19] B. Barwick, D. J. Flannigan, and A. H. Zewail. Photon-induced near-field electron microscopy. *Nature*, 462:902–906, 2009.

[20] L. Allen, M. W. Beijersbergen, R. J. C. Spreeuw, and J. P. Woerdman. Orbital angular momentum of light and the transformation of laguerre–gaussian laser modes. *Physical Review A*, 45:8185–8189, 1992.